SCIENCE CHINA
Life Sciences

THEMATIC ISSUE: Stem cells and regenerative medicine in China
• RESEARCH PAPER •

February 2014 Vol.57 No.2: 181–187
doi: 10.1007/s11427-014-4610-9

Biocompatibility of nano-hydroxyapatite/Mg-Zn-Ca alloy composite scaffolds to human umbilical cord mesenchymal stem cells from Wharton's jelly *in vitro*

GUAN FangXia[1,2], MA ShanShan[1], SHI XinYi[1,3], MA Xun[4], CHI LianKai[1], LIANG Shuo[1], CUI YuanBo[1], WANG ZhiBin[1], YAO Ning[1], GUAN ShaoKang[4*] & YANG Bo[5*]

[1]*School of Life Sciences, Zhengzhou University, Zhengzhou 450001, China;*
[2]*The First Affiliated Hospital of Zhengzhou University, Zhengzhou 450052, China;*
[3]*Interventional Hospital of Shandong Red Cross Society, Jinan 250014, China;*
[4]*Materials Research Center, School of Materials Science and Engineering, Zhengzhou University, Zhengzhou 450002, China;*
[5]*Department of Neurosurgery, The First Affiliated Hospital of Zhengzhou University, Zhengzhou 450052, China*

Received August 7, 2013; accepted October 16, 2013; published online January 17, 2014

Seeding cells and scaffolds play pivotal roles in bone tissue engineering and regenerative medicine. Wharton's jelly-derived mesenchymal stem cells (WJCs) from human umbilical cord represent attractive and promising seeding cells in tissue regeneration and engineering for treatment applications. This study was carried out to explore the biocompatibility of scaffolds to seeding cells *in vitro*. Rod-like nano-hydroxyapatite (RN-HA) and flake-like micro-hydroxyapatite (FM-HA) coatings were prepared on Mg-Zn-Ca alloy substrates using micro-arc oxidation and electrochemical deposition. WJCs were utilized to investigate the cellular biocompatibility of Mg-Zn-Ca alloys after different surface modifications by observing the cell adhesion, morphology, proliferation, and osteoblastic differentiation. The *in vitro* results indicated that the RN-HA coating group was more suitable for cell proliferation and cell osteoblastic differentiation than the FM-HA group, demonstrating better biocompatibility. Our results suggested that the RN-HA coating on Mg-Zn-Ca alloy substrates might be of great potential in bone tissue engineering.

nano-hydroxyapatite, Mg-Zn-Ca alloy, mesenchymal stem cells, Wharton's jelly, biocompatibility

Citation: Guan FX, Ma SS, Shi XY, Ma X, Chi LK, Liang S, Cui YB, Wang ZB, Yao N, Guan SK, Yang B. Biocompatibility of nano-hydroxyapatite/Mg-Zn-Ca alloy composite scaffolds to human umbilical cord mesenchymal stem cells from Wharton's jelly *in vitro*. Sci China Life Sci, 2014, 57: 181−187, doi: 10.1007/s11427-014-4610-9

Seeding cells and scaffolds serving as matrices for tissue formation play pivotal roles in bone tissue engineering and regenerative medicine. Bone marrow stem cells (BMSCs) are the most common seeding cells in tissue engineering, although some disadvantages, such as derivation from injury and smaller cell numbers obtained from the elderly, limit their clinical application. In recent years, Wharton's jelly-derived mesenchymal stem cells from human umbilical cord (WJCs) have received increasing interest [1]. WJCs possess multipotent properties and can be successfully differentiated into mature adipocytes, osteoblasts, chondrocytes, skeletal myocytes, cardiomyocytes, neurons, and endothelial cells. In contrast to bone marrow MSCs, WJCs have greater expansion capability *in vitro*, and WJCs are immune suppressive in allogenic transplant [2]. WJCs represent an attractive and promising field in tissue regeneration and engineering for treatment applications in a wide range of trauma and orthopedic conditions. Therefore, it is

*Corresponding author (email: yangbo96@126.com; skguan@zzu.edu.cn)

necessary to study cell responses under *in vitro* conditions using WJCs at the interface.

Recently, magnesium alloys have attracted extensive attention as biodegradable metallic implants due to their biodegradability in the bioenvironment, and their excellent mechanical properties, such as high strength and an elastic modulus close to that of bone [3–5]. Bone mineral is mainly composed of hydroxyapatite (HA, $Ca_5(PO_4)_3OH$), which is in the form of nanocrystals with dimensions of about 4 nm× 50 nm×50 nm [6,7]. Thus, HA has excellent biocompatibility and bioactivity, and has been widely developed as a coating on metallic substrates for bio-application [8]. Therefore, fabricating a nano-sized HA coating on the micro-arc oxidation (MAO) coating may be a promising way to improve the biocompatibility and corrosion resistance of magnesium alloys [9,10]. Also, recent developments in biomineralization have already demonstrated that nano-sized crystals and particles are considered to be important for the formation of hard tissues in animals [11]. The nano-sized HA can promote bone cell adhesion and osteoblastic proliferation in comparison with micro-sized HA [12–14]. However, there are still controversies about cytocompatability of nano-HA, given reports that nano-HA displayed evident cellular toxicity, and imposed restrictions on cell growth and differentiation [15,16].

Until now, related results about the response of human WJCs to biodegradable HA have not been reported. In our study, WJCs were isolated and characterized, and rod-like nano-hydroxyapatite (RN-HA) and flake-like micro-hydroxyapatite (FM-HA) coatings were prepared on Mg-Zn-Ca alloy substrates using MAO and electrochemical deposition (ED). First, WJCs at passage three were seeded onto the sterilized composite scaffolds in the osteogenic culture medium. Then, we investigated the cytocompatibility of RN-HA coatings and FM-HA coatings with WJCs seeded on by different methods. The adhesion and proliferation of WJCs were evaluated using phase-contrast microscopy, scanning electron microscopy (SEM) and CCK-8 assay. Finally, the differentiation of WJCs into osteoblastic cell phenotype was examined by a series of assays including alizarin red staining, Von Kossa staining, osteopontin (OPN) immunohistochemical staining, alkaline phosphatase (ALP) test and RT-PCR. Thus, we analyzed the biocompatibility of nano-hydroxyapatite/Mg-Zn-Ca alloy composite scaffolds to human WJCs *in vitro*, which may provide an important reference for clinical applications.

1 Materials and methods

1.1 Surface modification and characterization

Mg-Zn-Ca alloy was chosen as the substrate to fabricate composite HA coatings. The detailed procedure for preparation of the composite coatings was described in our previous work [9,17]. The surface morphology and elemental compositions of the coatings were investigated with a Quanta-200 SEM equipped with energy dispersion spectroscopy (EDS) capability.

1.2 Cell culture

In experiments approved by the Research Ethics Committee of Zhengzhou University, samples of human umbilical cord were obtained from the healthy donors under sterile condition. Detailed procedures were as previously described [10].

1.3 Cell morphology

WJCs at passage three were seeded onto each specimen at a seeding density of 1×10^4/ disk and divided into two groups: FM-HA group (with FM-HA coating) and RN-HA group (with RN-HA coating). Cell adhesion to the materials was observed by phase-contrast microscopy and SEM. Detailed procedures were as previously described [10].

1.4 Cell proliferation

WJCs at passage three were seeded on groups A and B at a density of 5×10^3/disk. After 24 h, the proliferation of WJCs was determined by CCK-8 assay according to the manufacturer's instructions. Subsequently, the optical density at 570 nm was evaluated using a micro-plate spectrophotometer. The assays were performed daily, and five wells were randomly taken into examination each time.

1.5 ALP tests

The WJCs at passage three were seeded onto two groups at a seeding density of 1×10^4/disk. On the second or third day, the culture medium was changed to induced medium, which was used to induce osteoblast differentiation with 50 mg L^{-1} ascorbic acid, 10 mol L^{-1} dexamethasone and 10 mmol L^{-1} β-glycerophosphate. The induced medium was changed every three days. ALP activity was measured by biochemical assay using the diagnostic kit according to the manufacturer's instructions, when WJCs were cultured for 7, 14, 21 d on different scaffolds. In the meantime, total protein content was determined by the Coomassie brilliant blue method. The ALP activity values were finally normalized based on corresponding protein concentrations.

1.6 Alizarin red staining and Von Kossa staining

After 14 days of culture, the WJCs were washed three times with PBS, and fixed in 4% paraformaldehyde (PFA) for 30 min. Fixed cells were incubated with 0.1% Alizarin red-Tris-HCl (pH 8.3) at 37°C for 30 min. In the end, the cells were also washed and coverslipped with glycogelatin. For Von Kossa staining, cells were fixed as for alizarin red staining, incubated with 2% $AgNO_3$ for 1 h in ultraviolet

light, washed three times, then incubated with 5% hyposulfite solution for 5 min. Finally, the results were viewed with an optical microscope.

1.7 Immunohistochemical staining

Osteopontin (OPN) expression was examined by immunohistochemical methods. Briefly, the WJCs were washed three times with PBS and were fixed in 4% PFA for 15 min, washed twice with PBS and incubated with 0.3% TritonX-100 for 30 min, after which the cells were immersed in 0.3% H_2O_2/methanol solution for 10 min and immunoblocked with 10% normal goat serum in PBS at room temperature for 30 min. Next, cells were incubated overnight with monoclonal rat anti-human OPN antibody at 4°C, then incubated with biotin-marked goat anti-mouse IgG for 30 min at 37°C and peroxide enzymeconjugated streptomycin avidin for 15 min at 37°C. After diaminobenzidine (DAB) coloration for 5 min and hematoxylin-eosin (HE) staining, the cells were washed with PBS, coverslipped and viewed with an optical microscope.

1.8 RT-PCR

After cultured for 21 d, the WJCs were collected for RNA isolation and gene expression analysis. Total RNA was isolated by using TRIzol (Invitrogen, USA) following manufacturer's instructions. The primers of osteoblastic differentiation-related genes were as follows: Runx2 forward 5′-TCCTATGACCAGTCTTACCCCT-3′ and reverse 5′-GGCTCTTCTTACTGAGAGTGGAA-3′; OPN forward 5′-CTGAACGCGCCTTCTGATTG-3′ and reverse 5′-ACATCGGAATGCTCATTGCTCT-3′; OCN forward 5′-GGCGCTACCTGTATCAATGGC-3′ and reverse 5′-TGCCTGGAGAGGAGCAGAACT-3′. β-Actin was utilized as an internal control, and the primers were 5′-CTCCATCCTGGCCTCGCTGT-3′ and 5′-GCTGTCACCTTCACCGTTCC-3′.

1.9 Statistical analysis

Quantitative data were presented as means±standard deviations (SD). Statistical analysis was assessed using SPSS (v17.0). A student's *t*-test (assuming equal variances) was performed to determine the statistical significance between experimental groups. $P<0.05$ was considered to be significantly different.

2 Results

2.1 Adhesion and proliferation of WJCs on different composite scaffolds

The biocompatibilities in cell adhesion and proliferation of the different composite scaffolds were evaluated *in vitro* by observing the behavior of the three-passage WJCs by phase-contrast microscopy and CCK-8 assay. The WJCs had attached and migrated through the pores in two groups at 24 h, while the number of the cells increased more in RN-HA group after 48 h (Figure 1A–D). During 4-d cell culture, the cell number in RN-HA group increased gradually in the first three days and began to decrease in the fourth day, while the cell number in FM-HA group increased after 2-d cell culture, and began to decrease in the third day. Meanwhile, the number of cells in RN-HA group was more than FM-HA group every day (Figure 1E). Our results demonstrated that the RN-HA coating enhanced the adhesion and proliferation of WJCs, which are *in vitro* noncytotoxic and biocompatible to cells.

2.2 SEM and EDS analysis

To directly examine the morphology of WJCs on different composite scaffolds, we evaluated the cells by SEM. The WJCs adhered to both of the coatings, but the cells in RN-

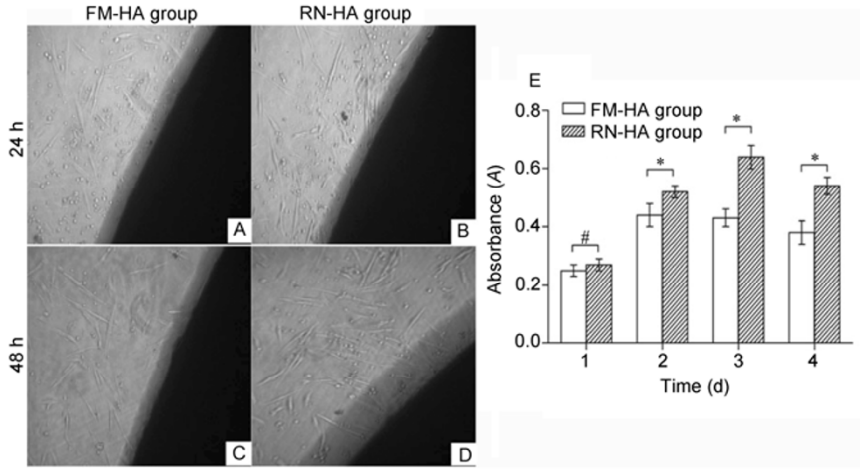

Figure 1 The adhesion and proliferation of WJCs on different composite scaffolds (×40). A–D, the adhesion of WJCs after different culture time in FM-HA and RN-HA group. E, Cell proliferation results according to absorbance values after 1–4 d incubation on the materials (mean±SD). *, $P<0.05$; #, $P>0.05$.

HA group were more adherent, the number of cells was also much larger compared with those in FM-HA group (Figure 2A and B). To further examine the growth morphology of cells, we found that the cells in FM-HA group demonstrated a small rounded morphology with no pseudopodia, and a large number of cells had no sign of growth, basically at apoptosis. The cells in RN-HA group were spread well in a large region of polygonal morphology and attached to the coating with several fine pseudopodia. In addition, numerous microvilli were grouped around the cells (Figure 2C and D). The WJCs in RN-HA group after cultured 48 h were also examined by SEM and found to be flat and well-spread on the surface (appeared black), with filopodia around the cells. Around the cells, numerous microvilli presented grouped on the top of the coating (the white cross in Figure 2E). A cross-section was analyzed by EDS (Figure 2F), which revealed a large amount of Ca, P, O and Mg, Na elements, suggesting that the microvilli were possibly calcium phosphate deposited during the cell culture process. These findings indicated that the RN-HA coating induced the deposition of calcium phosphate, demonstrating better biocompatibility.

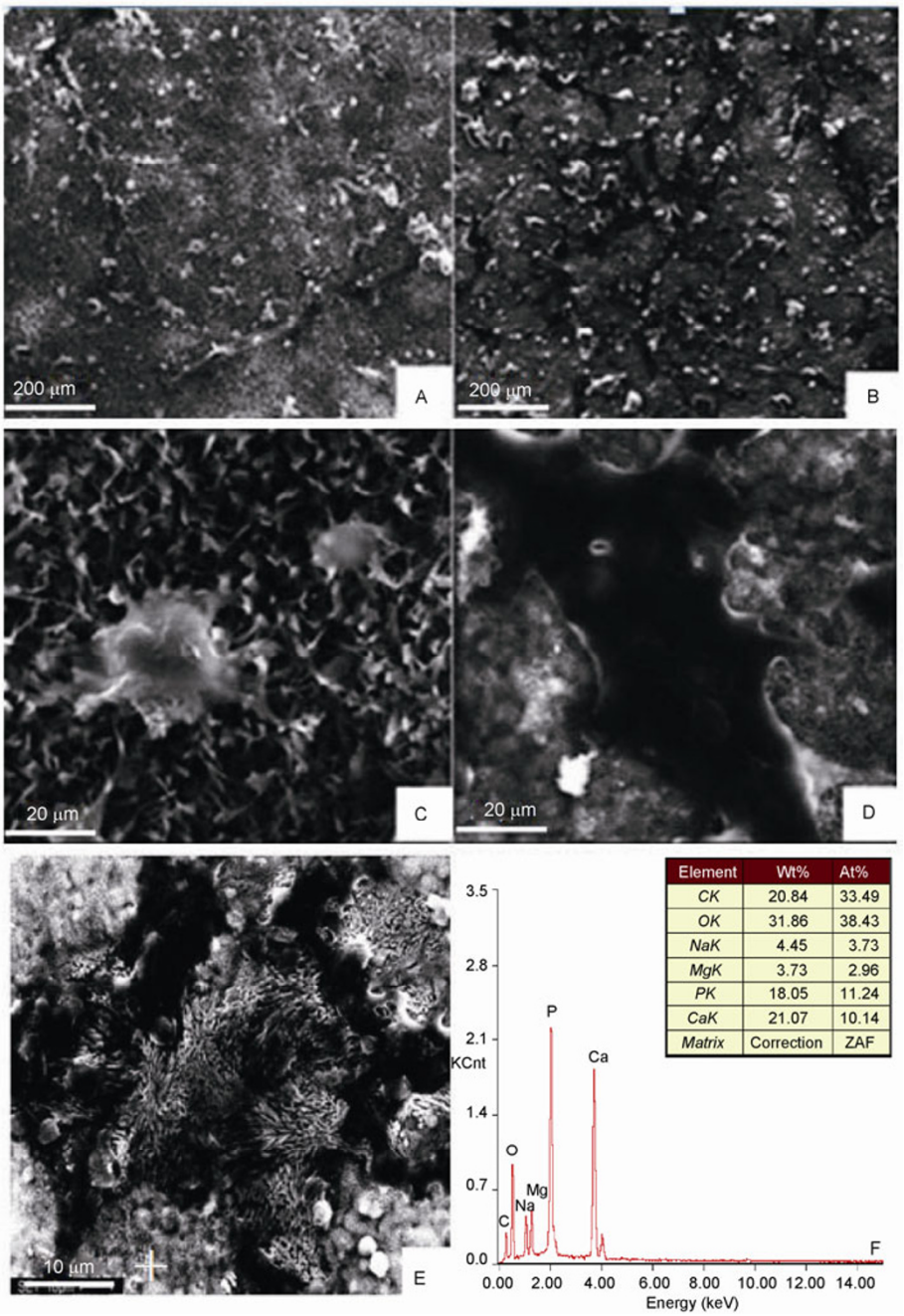

Figure 2 The morphology of WJCs seeded on different scaffolds. A and C, FM-HA coating after 24 h. B and D, RN-HA coating after 24 h. E and F, the SEM images and EDS spectra of WJCs on RN-HA coating and cultivated for 48 h.

2.3 Biocompatibility in cell differentiation

Alkaline phosphatase (ALP), calcium deposition and osteopontin (OPN) are the landmarks of mature osteoblast, which were examined by different methods to analyze the cell differentiation. At day 7 incubation of WJCs/scaffold constructs with osteogenic stimulation, low ALP activity was detected, indicating that few stem cells were differentiated into osteoblast cells. With prolonged incubation period, the level of ALP activity increased substantially in all samples, with the ALP activity from RN-HA group continually higher than that from FM-HA group (Figure 3A). Also, positive staining of alizarin red and Von Kossa, which were used to detect the calcium deposition, were observed (Figure 3B and C), indicating the osteogenic differentiation of WJCs into osteoblasts. Meanwhile, OPN was expressed after incubation of WJCs/ RN-HA coating constructs in osteogenic medium for 14 d (Figure 3D and E). These results demonstrated that RN-HA/Mg-Zn-Ca alloy had no detectable negative effects on WJCs osteogenic differentiation, but enhanced WJCs osteoblastic differentiation to some degree.

2.4 The expression of osteoblastic markers by RT-PCR analysis

To detect cell differentiation at the molecular level, we analyzed the expression of osteoblastic differentiation markers such as OPN, OCN and Runx2 by RT-PCR. On day 21, OPN and OCN were expressed in both FM-HA group and RN-HA group, while Runx2 was expressed only in RN-HA group. Notably, WJCs exhibited pronounced signals of all the markers mentioned above while being cultured in RN-HA group for 21 d (Figure 4).

3 Discussion

Our work demonstrated that WJCs grew and spread better in RN-HA group, suggesting better cell viability. More filopodia occurred to facilitate the interactions between cells and substrates as well as among cells themselves, and more confluences and connections among cells occurred in RN-HA group. CCK-8 assay indicated that the proliferation proceeded more significantly in RN-HA group after three days of incubation. These results suggested that in RN-HA coating enhanced the attachment and proliferation of WJCs, which are *in vitro* noncytotoxic and biocompatible with cells. This may be attributed to attributes of RN-HA coatings as compared to FM-HA coatings, such as the surface structure [18]. The higher crystallinity and density of the RN-HA coating could improve cell attachment and growth as seen with the SEM and phase-contrast microscopy. The compactness and crystallinity of the FM-HA coating were

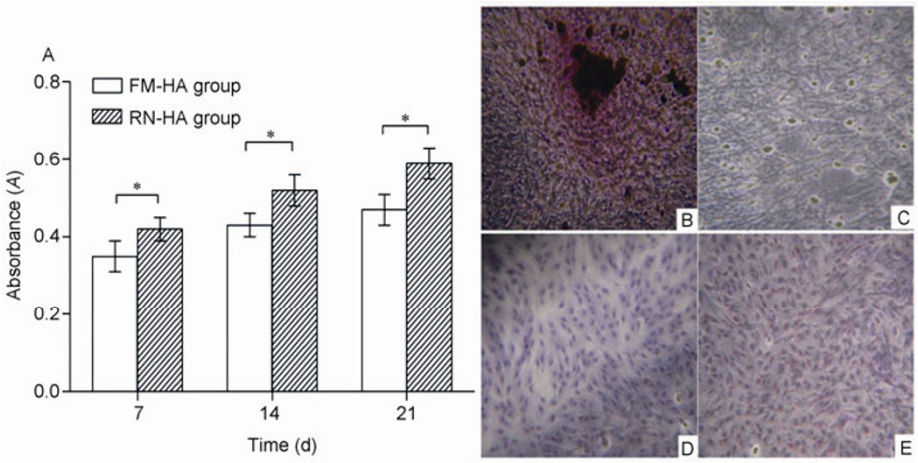

Figure 3 Cell differentiation. A, ALP levels quantified of WJCs cultured in FM-HA group and RN-HA group (mean±SD). B, Alizarin red staining of the cells at third generation cultured with ossification additive for 14 d (×100). C, Von Kossa staining with ossification additive for 14 d (×40). D and E, OPN expression after WJCs cultured with scaffold for 14 d (×40, D: Negative; E: Positive). *, $P< 0.05$.

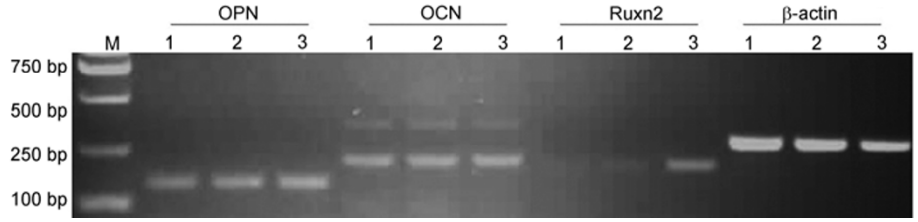

Figure 4 RT-PCR analysis of the expression of osteoblastic markers. M: marker; 1: the cell group; 2: FM-HA group; 3: RN-HA group.

lower, therefore a cell could only come into contact with the top of a few flake-like grains of hydroxyapatite, leaving most of the cell wall hanging in air. Okada et al. pointed out that the formation of focal adhesion requires a flat domain size larger than 100 nm in width [19]. Massive cell apoptosis found on the FM-HA coating may be attributed to the coating barely meeting this requirement. In addition, lower compactness could result in the medium seeping deep into the coating, so that dissolution of magnesium ions and rapid increase in medium pH occurred [20,21]. During the experiment, the pH value in the cell culture medium of the FM-HA coating increased rapidly during cell growth, resulting in poor growth conditions. However, the RN-HA coating whose grains were arranged in regular and consistent orientation had a dense compactness providing sufficient contact area for cell adhesion, growth and better coating corrosion resistance. Futhermore, there were numerous microvilli present on top of the RN-HA coating, but not on the FM-HA coating. This observation combined with energy spectrum analysis, suggests that the microvilli were possibly calcium phosphate deposited during the cell culture process, indicating that the RN-HA coating induced the deposition of calcium phosphate, resulting in better biocompatibility.

At the protein level, the differentiation of WJCs into osteoblastic phenotype were analyzed by ALP activity and OPN immunohistochemical staining, which were important factors in qualitatively determining bone differentiation and mineralization [22–24]. The results of ALP activity indicated that RN-HA coating supported osteoblastic differentiation of WJCs to a higher degree. As staining results revealed, WJCs in direct contact with RN-HA /Mg-Zn-Ca scaffold exhibited positive expression for OPN. The deposition of calcium-containing mineral after WJCs' osteoblastic differentiation was observed using alizarin red staining and von Kossa staining. All the results above demonstrated that the RN-HA coating material had less negative influence on WJCs' osteoblastic differentiation, and somewhat enhanced WJCs' osteoblastic differentiation. Compared to FM-HA, RN-HA was proved to enhance the osteoblastic differentiation of WJCs, the synthesis of intracellular proteins, the alkaline phosphatase activity and the deposition of calcium-containing mineral, thus enhancing the bonding of orthopedic/dental implants to juxtaposed bone and improving the overall implant efficacy [25, 26].

Finally, at the molecular level, OPN, OCN and Runx2 were demonstrated to be expressed during the later extracellular-matrix mineralization [27–33]. RT-PCR revealed that the expression of OPN and OCN had no clear difference between the two groups. The significantly higher level of Runx2 expressions occurred in RN-HA group, while none occurred in FM-HA group. Considering the Runx2 protein, which was thought to be an essential bone maturation factor [34], the RN-HA coating enhanced the WJCs expression after 21 days of osteogenic culture. This revealed that the RN-HA coatings were able to facilitate the expression of bone-related transcription factors such as Runx2 to drive MSCs' differentiation along the osteoblastic pathway. Generally, the *in vitro* results indicated that the RN-HA group was more suitable for cell proliferation and cell osteoblastic differentiation than the FM-HA group, which was more important for *in vivo* implantation.

This work was supported by the National Natural Science Foundation of China (81071008, 81171177, and 30870634), the Strategic Priority Research Program of the Chinese Academy of Sciences (XDA01030300), the Program for New Century Excellent Talents in University (NCET-06-0611), the Excellent Youth Foundation of Henan Scientific Committee (114100510005), the Young Excellent Teachers in University Funded Projects of Henan Province, and Bureau of Science and Technology Development Project from Henan Province (122102310203).

1 Can A, Karahuseyinoglu S. Concise review: human umbilical cord stroma with regard to the source of fetus-derived stem cells. Stem Cells, 2007, 25: 2886–2895
2 Troyer DL, Weiss ML. Wharton's jelly-derived cells are a primitive stromal cell population. Stem Cells, 2008, 26: 591–599
3 Witte F, Hort N, Vogt C, Cohen S, Kainer KU, Willumeit R, Feyerabend F. Degradable biomaterials based on magnesium corrosion. Curr Opin Solid St M , 2008, 12: 63–72
4 Zhang S, Zhang X, Zhao C, Li J, Song Y, Xie C, Tao H, Zhang Y, He Y, Jiang Y, Bian Y. Research on an Mg-Zn alloy as a degradable biomaterial. Acta Biomater, 2010, 6: 626–640
5 Zheng YF, Gu XN, Xi YL, Chai DL. *In vitro* degradation and cytotoxicity of Mg/Ca composites produced by powder metallurgy. Acta Biomater, 2010, 6: 1783–1791
6 Lowenstam HA, Weiner S. On biomineralization. Oxford: Oxford University Press, 1989
7 McConnell D. The crystal structure of bone. Clin Orthop, 1962, 23: 253–268
8 Huang Y, Qu Y, Yang B, Li W, Zhang B, Zhang X. *In vivo* biological responses of plasma sprayed hydroxyapatite coatings with an electric polarized treatment in alkaline solution. Mater Sci Eng C, 2009, 29: 2411–2416
9 Gao J, Guan S, Chen J, Wang L, Zhu S, Hu J, Ren Z. Fabrication and characterization of rod-like nano-hydroxyapatite on mao coating supported on Mg-Zn-Ca alloy. Appl Surf Sci, 2011, 257: 2231–2237
10 Gao J, Shi X, Yang B, Hou S, Meng E, Guan F, Guan S. Fabrication and characterization of bioactive composite coatings on Mg-Zn-Ca alloy by MAO/sol–gel. J Mater Sci: Mater in Med, 2011, 22: 1681–1687
11 Dorozhkin SV. Nanosized and nanocrystalline calcium orthophosphates. Acta Biomater, 2010, 6: 715–734
12 Bose S, Dasgupta S, Tarafder S, Bandyopadhyay A. Microwave-processed nanocrystalline hydroxyapatite: Simultaneous enhancement of mechanical and biological properties. Acta Biomater, 2010, 6: 3782–3790
13 Lu YP, Chen YM, Li ST, Wang JH. Surface nanocrystallization of hydroxyapatite coating. Acta Biomater, 2008, 4: 1865–1872
14 Wang J, Shaw LL. Nanocrystalline hydroxyapatite with simultaneous enhancements in hardness and toughness. Biomaterials, 2009, 30: 6565–6572
15 Li J, Yin Y, Yao F, Zhang L, Yao K. Effect of nano-and micro-hydroxyapatite/chitosan-gelatin network film on human gastric cancer cells. Mater Lett, 2008, 62: 3220–3223
16 Roy M, Bandyopadhyay A, Bose S. Induction plasma sprayed nano hydroxyapatite coatings on titanium for orthopaedic and dental implants. Surf Coat Technol, 2011, 205: 2785–2792
17 Li W, Guan S, Chen J, Hu J, Chen S, Wang L, Zhu S. Preparation

and in vitro degradation of the composite coating with high adhesion strength on biodegradable Mg-Zn-Ca alloy. Mater Charact , 2011, 62: 1158–1165
18 Matsumoto T, Okazaki M, Inoue M, Yamaguchi S, Kusunose T, Toyonaga T, Hamada Y, Takahashi J. Hydroxyapatite particles as a controlled release carrier of protein. Biomaterials, 2004, 25: 3807–3812
19 Okada S, Ito H, Nagai A, Komotori J, Imai H. Adhesion of osteoblast-like cells on nanostructured hydroxyapatite. Acta Biomater, 2010, 6: 591–597
20 Kandori K, Saito M, Saito H, Yasukawa A, Ishikawa T. Adsorption of protein on non-stoichiometric calcium-strontium hydroxyapatite. Colloid Surface A, 1995, 94: 225–230
21 Sharpe J, Sammons R, Marquis P. Effect of pH on protein adsorption to hydroxyapatite and tricalcium phosphate ceramics. Biomaterials, 1997, 18: 471–476
22 Kang MI, Lee WY, Oh KW, Han JH, Song KH, Cha BY, Lee KW, Son HY, Kang SK, Kim CC. The short-term changes of bone mineral metabolism following bone marrow transplantation. Bone, 2000, 26: 275–279
23 Marom R, Shur I, Solomon R, Benayahu D. Characterization of adhesion and differentiation markers of osteogenic marrow stromal cells. J Cell Physiol, 2005, 202: 41–48
24 Stucki U, Schmid J, Hammerle CF, Lang NP. Temporal and local appearance of alkaline phosphatase activity in early stages of guided bone regeneration. A descriptive histochemical study in humans. Clin Oral Implant Res, 2001, 12: 121–127
25 Elias KL, Price RL, Webster TJ. Enhanced functions of osteoblasts on nanometer diameter carbon fibers. Biomaterials, 2002, 23: 3279–3287
26 Webster TJ, Ergun C, Doremus RH, Siegel RW, Bizios R. Enhanced functions of osteoblasts on nanophase ceramics. Biomaterials, 2000, 21: 1803–1810
27 Aubin JE. Advances in the osteoblast lineage. Biochem Cell Biol, 1998, 76: 899–910
28 Franceschi RT. The developmental control of osteoblast-specific gene expression: Role of specific transcription factors and the extracellular matrix environment. Crit Rev in Oral Biol Med, 1999, 10: 40–57
29 Knabe C, Berger G, Gildenhaar R, Klar F, Zreiqat H. The modulation of osteogenesis in vitro by calcium titanium phosphate coatings. Biomaterials, 2004, 25: 4911–4919
30 Morinobu M, Ishijima M, Rittling SR, Tsuji K, Yamamoto H, Nifuji A, Denhardt DT, Noda M. Osteopontin expression in osteoblasts and osteocytes during bone formation under mechanical stress in the calvarial suture in vivo. J Bone Miner Res, 2003, 18: 1706–1715
31 Satomura K, Krebsbach P, Bianco P, Gehron Robey P. Osteogenic imprinting upstream of marrow stromal cell differentiation. J Cell Biochem, 2000, 78: 391–403
32 Sodek J, Zhang Q, Goldberg H, Domenicucci C, Kasugai S, Wrana J, Shapiro H, Chen J. Non-collagenous bone proteins and their role in substrate-induced bioactivity. In: Davies JE, eds. The Bone-Biomaterial Interface. Toronto: University of Toronto Press, 1991. 97–110
33 Frank O, Heim M, Jakob M, Barbero A, Schafer D, Bendik I, Dick W, Heberer M, Martin I. Real-time quantitative RT-PCR analysis of human bone marrow stromal cells during osteogenic differentiation in vitro. J Cell Biochem, 2002, 85: 737–746
34 Vitolo MI, Anglin IE, Mahoney WM Jr., Renoud KJ, Gartenhaus RB, Bachman KE, Passaniti A. The RUNX2 transcription factor cooperates with the YES-associated protein, YAP65, to promote cell transformation. Cancer Biol Ther, 2007, 6: 856–863